Biomimetic Separation of Transport and Matrix Functions in Lamellar Block Copolymer Channel-Based Membranes

Chao Lang^{a,b}, Dan Ye^a, Woochul Song^a, Chenhao Yao^a, Yu-ming Tu^a, Clara Capparelli^{a,b}, Jacob A. LaNasa^b, Michael A. Hickner^{b,e}, Esther W. Gomez^{a,c}, Enrique D . Gomez^{a,b,e}, Robert J. Hickey*,b,e</sup>, Manish Kumar*,a,c,d,e

Department of Chemical Engineering, ^b Department of Materials Science & Engineering, ^c
 Department of Biomedical Engineering, ^d Department of Civil and Environmental Engineering, ^e
 Materials Research Institute, The Pennsylvania State University, University Park, PA, 16802 USA

Abstract: Cell membranes control mass, energy, and information flow to and from the cell. In the cell membrane a lipid bilayer serves as the barrier layer, with highly efficient molecular machines, membrane proteins, serving as the transport elements. In this way, highly specialized transport properties are achieved by these composite materials by segregating the matrix function from the transport function using different components. For example, cell membranes containing aggaporin proteins can transport four billion water molecules per second per aquaporin while rejecting all other molecules including salts - a feat unmatched by any synthetic system, while the impermeable lipid bilayer provides the barrier and matrix properties. True separation of functions between the matrix and the transport elements has been difficult to achieve in conventional solute separation synthetic membranes. In this study, we created membranes with distinct matrix and transport elements through designed co-assembly of solvent-stable artificial (peptide appended pillar[5] arene, PAP5) or natural (gramicidin A) model channels with block copolymers into lamellar multilayered membranes. Selfassembly of a lamellar structure from crosslinkable triblock copolymers was used as a scalable replacement for lipid bilayers, offering better stability and mechanical properties. By co-assembly of channel molecules with block copolymers, we were able to synthesize nanofiltration membranes with sharp selectivity profiles as well as uncharged ion exchange membranes exhibiting ion selectivity. The developed method can be used for incorporation of different artificial and biological ion and water channels into synthetic polymer membranes. The strategy reported here could promote the construction of a range of channel-based membranes and sensors with desired properties, such as ion separations, stimuli responsiveness, and high sensitivity.

Keywords: membrane; artificial channel; pillar[5]arene; self-assembly; block copolymer; lamellae

A long-standing challenge in membrane separations is the selectivity-permeability "tradeoff" - a phenomenon that prevents membranes from simultaneously exhibiting both high selectivity and high permeability. ADDIN EN.CITE 1-4 However, in nature, this trade-off is elegantly overcome through specialized transport proteins. ADDIN EN.CITE 5-7 In biological membranes, there is a clear division of labor between components with the matrix support function (lipid bilayers) and the transport function (membrane proteins). This separation is not seen in current polymeric membranes where the matrix and the transport elements consist of the same material in a vast majority of cases.3 Due to the uniform structure and chemical identity of each transport membrane protein, biological membranes exhibit molecularly selective transport, which is challenging to achieve in current polymeric

membranes.8 The transport elements (pores for porous membranes or free volume elements for non-porous solution diffusion membranes) of current commercial membranes vary greatly in size, shape and pore lining functional groups, which leads to a broad separation range instead of a single separation "cut-off".9 As a result, separation profiles for traditional membranes are broad at any nominal pore size. Beyond separations, an increasing number of technologies based on membrane proteins and nanopores are being developed, ADDIN EN.CITE 10 -14 and suitable matrices could enable faster adoption and proliferation of biological and artificial channel-based technologies. A prime example of a successful channel-based technology is the low cost nanopore genetic sequencer, MinION from Oxford Nanopore technologies, which is based on the membrane

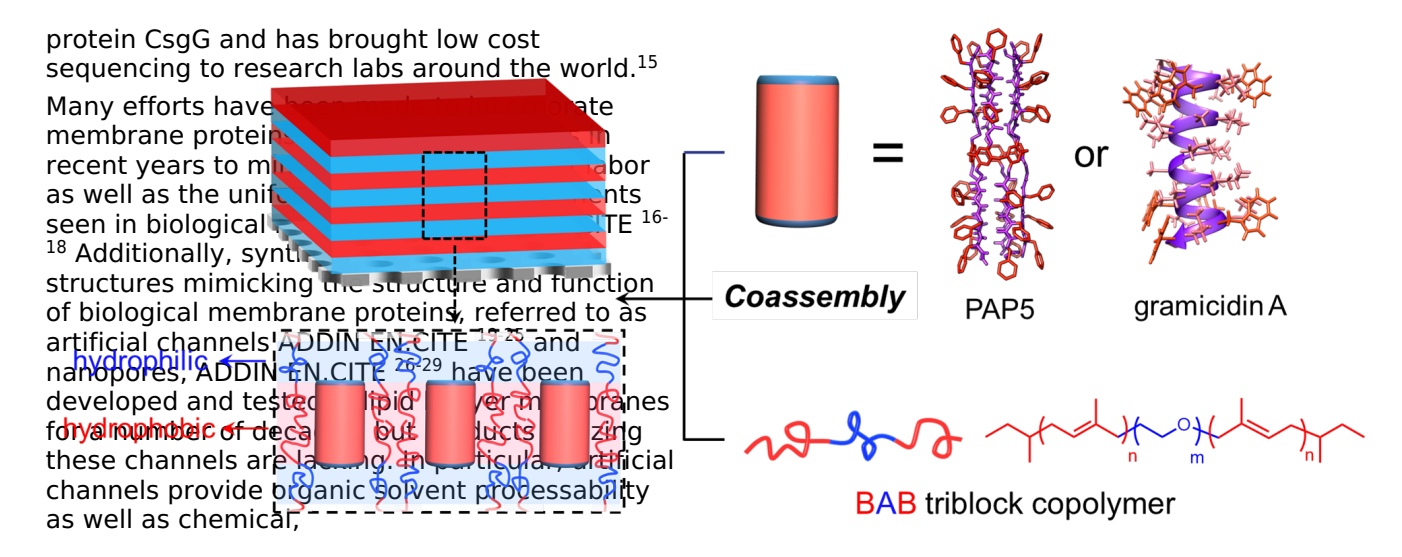


Figure 1. Schematic illustration of the developed platform for channel-based membranes using a self-assembled lamellar block copolymer matrix. Pillar[5]arene-based artificial channels or natural cation channel gramicidin A were co-assembled with BAB triblock copolymers consisting of hydrophilic middle A -block and hydrophobic end B-blocks to form membranes exhibiting distinct separation performance determined by the incorporated channel elements. In the study, block copolymers are referred as BA(n-m) or BAB(n-m-n), where n and m are number-average molecular weights (kg/mol) of B and A block respectively. Detailed molecular information on the polymers is shown in **Table 1**.

mechanical, and biological stability that may be challenging to achieve in most biological channels. ADDIN EN.CITE ³⁰⁻³² Despite the clear advantages of membrane proteins and their mimics in potential technologies, development of membranes around artificial and biological channels is still at an incipient stage. A major hurdle is that most of these channels are tested in and designed for use in lipids that are not generally considered stable engineering materials for larger scale applications.³³

In the search for suitable replacements for lipids, block copolymers have emerged as excellent candidates. ADDIN EN.CITE 17, 34-40 By covalently connecting incompatible polymer blocks together, block copolymers can be used to simulate the amphiphilic structure of lipid bilavers for channel incorporation. For instance, ABA triblock copolymer poly(2-methyloxazoline)-blockpoly(dimethylsiloxane)-block-poly(2methyloxazoline) (PMOXA-PDMS-PMOXA), where A is hydrophilic and B is hydrophobic, has been widely explored in the incorporation of water channel protein Aquaporin Z.34 Poly(butadiene)block-poly(ethylene oxide) (BO) is another suitable candidate for channel insertions. including both membrane proteins,17 and artificial channel peptide-appended pillar[5]arene (PAP5)41 to form 2D nanosheets. In addition, block copolymer nanostructures ADDIN EN.CITE 42-45 and liquid crystalline mesophases ADDIN EN.CITE ⁴⁶⁻⁴⁸ have already shown great potential in fabricating self-assembled membrane materials. ADDIN EN.CITE 49-51 It has been shown that with block copolymers ADDIN EN.CITE 52-58 or polymerizable oligomers, ADDIN EN.CITE 46-48 well -ordered membranes with pore size in the range of a few to several hundred nanometers can be

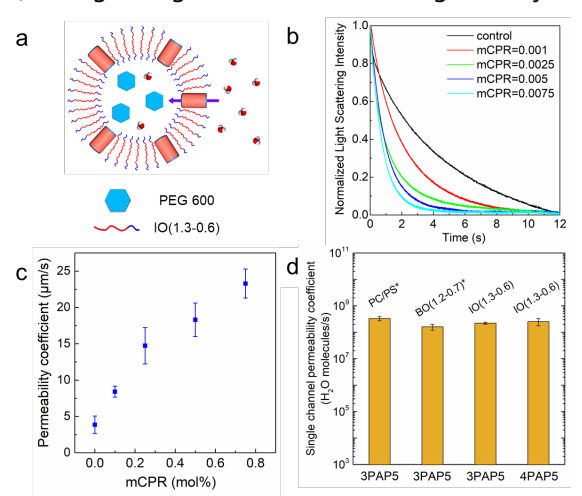
prepared. Although for such membranes pore sizes in the 1-3 nm range are achievable, ADDIN EN.CITE ⁵⁹⁻⁶¹ it is a challenging task to further decrease the pore size.^{49, 62} By introducing artificial and biological channels, porous membranes with sub-nanometer sized pores can be realized. A simple platform for incorporating artificial and biological channels is critical to the development of high performance channel based membranes.⁶³

A few platforms for incorporating channels in membranes have been reported but suffer from multi-step processing procedures. 63 One promising strategy is to incorporate channelinserted vesicles into the selective layer of existing membranes. This has been widely explored with Aquaporin (AQP) channels for the permeability improvement of reverse osmosis membranes.^{5, 34} Another notable way to make channel based membranes is the deposition of channel-based 2D crystals using a layer-by-layer method. ADDIN EN.CITE 9, 41, 64 where artificial channels are co-assembled with diblock copolymers to form flat-sheet like 2D crystals through a dialysis process. Finally, a hexagonally packed cylinder (HEX) structured block copolymer membrane with artificial channels inside membrane cylindrical domains has also been proposed. 65 Å supramolecular channel from selfassembled cyclic peptide was incorporated into the cylindrical domain of block copolymer matrix, leading to the formation of porous thin film with proton transport abilities. 65 All of these methods require preparation of self-assembled structures that can take several days and stringent control over the process. Additionally, in most cases the process of self-assembly is isolated from membrane fabrication, making it difficult for the

process to be replicated at larger scales.

In order to develop a more general and easily adaptable platform for channel based membranes , we targeted the lamellar morphology, which is a common nanostructure that forms via the selfassembly of block copolymers, as a next generation model system. 63, 66 Reminiscent of lipid bilayers, the lamellar structure made from amphiphilic block copolymer consists of alternating hydrophilic and hydrophobic layers (Figure 1). Thus, inserted artificial channels naturally align normal to the lamellar plane in order to match hydrophilic channel ends and hydrophobic channel body to corresponding lamellar layers. By using a somewhat counter intuitive BAB triblock copolymer design, where A represents the hydrophilic block and B represents crosslinkable hydrophobic blocks, we were able to create a

multilayer lamellar matrix that resists delamination when contacted with water (Figure 1. S1). The hydrophobic end B blocks initially serve as physical crosslinks when A block bridges two hydrophobic domains. It is worth noting that looping BAB chains in which B blocks reside in the same hydrophobic domain will not contribute as physical crosslinks. Furthermore, AB or ABA chain architectures will not form physical crosslinks, which will lead to delamination of the lamellar hydrophilic domains (Figure S1). To further increase the mechanical strength of the membrane, the hydrophobic domains were chemically crosslinked through click chemistry. Therefore, a chemically and physically crosslinked block copolymer matrix serving as an impermeable barrier with orientated artificial or natural channels inserted as separation elements can then be established as a platform for building various types of channel-based membranes. To demonstrate the practicality of the platform, triblock polymer poly(isoprene)-block-poly(ethylene oxide)-block-poly(isoprene) was chosen as matrix material with PAP5 and gramicidin A (a natural peptide channel) as model channels for membrane fabrication. Atomic Force Microscopy (AFM) and grazing-incidence small angle X-ray



scattering (GISAXS) were used to confirm the parallel orientated lamellar structure of the membrane matrix. Self-supporting membranes with thicknesses of approximately 90 nm were successfully constructed and transferred onto porous aluminum oxide substrate to form a composite membrane. Filtration and electrochemical separation tests shown that channel-incorporated membranes demonstrated distinct separation performance determined by the channel elements (**Figure 1**).

RESULTS AND DISCUSSION

In this paper, I (or PI), O (or PEO) and B (or PB) are abbreviations for poly(isoprene), poly(ethylene oxide) and poly(butadiene), respectively

. To explore the feasibility of using PI as the hydrophobic block and PEO as the hydrophilic block for making channel accommodation matrix. IO based block copolymer vesicles with PAP[5] channels incorporated were first tested using a well-established vesicle-based transport assay -stopped-flow light scattering. ADDIN EN.CITE ^{34, 41} Vesicles of uniform size were first prepared using the film hydration method⁶⁷ with diblock copolymer IO(1.3-0.6), where the hydration buffer contains 100 mM PEG600 and 25 mM NaCl (Figure S7). Upon rapid mixing with 25 mM NaCl water solution lacking PEG600, an inwardly directed osmotic pressure was established (vesicles under hypertonic conditions), leading to water influx into vesicles and thus vesicles swell. The osmotic permeability coefficient of the membrane can be then obtained by fitting the scattering intensity changing profile at a 90° angle (which decreases with increasing vesicle volume)68 according to time. The osmotic permeability coefficient of pure polymer vesicle membrane was first examined as the control (Figure 2b). It was found that compared to the previously reported BO system, IO showed better barrier properties (a osmotic permeability coefficient of 3.9 µm/s for IO(1.3-0.6) vesicles compared with 17.3 µm/s for BO(1.2-0.7) vesicles).9 Two types of pillar[5]arene-based channels with different peptide lengths, 3PAP5 (tripeptide sidechains) and 4PAP5 (tetrapeptide sidechains), were first synthesized (see detailed characterization data in supporting information. Figure S2-S5) and then tested in IO vesicles at various concentrations. As the added channel concentration increased (represented by the molar channel-to-polymer ratios, mCPR), the osmotic permeability coefficient of the membrane increased significantly (Figure 2b, 2c, S8). Noticeably, the increase in vesicle osmotic permeability coefficient with PAP5 channel is much more prominent with IO than with BO. At mCPR = 0.5%, 3PAP5 increases the osmotic permeability coefficient of IO(1.3-0.6) vesicle by 14.4 µm/s when compared to 3.3 µm/s for BO(1.2 -0.7) vesicle. To gain a deeper understanding of this difference, fluorescence correlation spectroscopy (FCS) was used to measure channel insertion efficiency (Figure S9). It was found the IO system demonstrated higher channel insertion values compared to BO system (1113 µm⁻² for 4PAP5 and 898 μm⁻² for 3PAP5 in IO(1.3-0.6) compared with 166 µm⁻² for 3PAP5 in BO(1.2-0.7) vesicles). The single channel permeability coefficient of both 3PAP5 and 4PAP5 tested in IO vesicles were comparable to that previously reported 3PAP5 in BO(1.2-0.7) and PC/PS lipid system (Figure 2d). Overall, vesicle-based characterization suggests that the IO block copolymer system is a suitable matrix to build

channel-based membrane based on its barrier properties and on its ability to maintain the efficiency and function of channel molecules.

Figure 2. Vesicle-based experiments for evaluating the feasibility of using IO as matrix for building channel-based membranes. (a) A scheme showing water transport through channels incorporated in IO vesicles under hypertonic conditions, which can be implemented using a stopped-flow system and vesicle size changes monitored using light scattering . (b) Stopped-flow curves showing the osmotic permeability coefficient of the IO(1.3-0.6) vesicle membrane increased significantly after 3PAP5 insertion. Vesicles with no channels were used as control. (c) Osmotic permeability coefficient values of IO(1.3-0.6) polymer vesicles with increased concentrations of 3PAP5 obtained by fitting the scattering intensity changing profile. (d) Single channel permeability coefficient of artificial channels in different systems: PC/PS (liposomes made from 4:1 mol/mol phosphatidylcholine/phosphatidylserine), BO(1.2-0.7) (*previously reported values)⁹ and IO(1.3-0.6) (values measured in this work).



0.15 = 0.15

] = 0.20

Table 1. Molecular weights, dispersity values, and poly(ethylene oxide) golume, Litesi ratios for the diblock and triblock [Li]:[EO] = 0.025 [Li]:[EO] = 0.05copolymers used in this study. [Li]:[EO] = 0.075-[Li]:[EO] = 0.10

Polymer ^a	M _{n,}	Ð ^c	f_{PEO}^{d}
IO(1.3-0.6)	kg/mol) 1.9	1.03	0.26
IOI(1.5-4.4-1.5	7.4	1.05	0.55
IOI(2.5-5.4-2.5)	10.4	1.03	0.46

^aIn the paper, poly(isoprene) and poly(ethylene oxide) are represented as I and O, respectively. b Total number-average molecular weights of block copolymers were determined using size-exclusion chromatography (SEC). CDispersity index ($\mathcal{D} = M_w/M_n$) was determined from SEC. dThe PEO volume fraction of the block copolymers were calculated using ¹H NMR data. The density values from MilliporeSigma were used, where the density of I is 0 .906 g mL $^{-1}$, and O is 1.13 g mL $^{-1}$ at 25 °C.

After establishing that IO can serve as a membrane matrix, we further synthesized IOI triblock copolymer by connecting IO diblock copolymer at the PEO ends to improve macroscopic membrane stability. The BAB triblock copolymers with two crosslinkable hydrophobic end blocks is more suitable for building channel-based membrane with lamellar morphology due to increased stability against delamination by swelling of hydrophilic blocks by water. Because the PEO blocks are not chemically linked, the hydrophilic domains of the lamellae from AB diblock copolymer are more likely to swell and cause lamellae to peel off into single layers even if the hydrophobic domain is crosslinked.

To obtain lamellar morphologies, IOI block copolymers with a PEO volume fraction of 50% was targeted. 43 The triblock copolymer was synthesized using sequential anionic polymerization followed by coupling the PEO ends of diblock copolymers.66 IOI triblock polymers of two different molecular weights (IOI(2.5-5.4-2.5) and IOI(1.5-4.4-1.5)) were synthesized. (Table 1, Figure S6)

A sacrificial layer assisted fabrication procedure was then adopted to fabricate lamellar

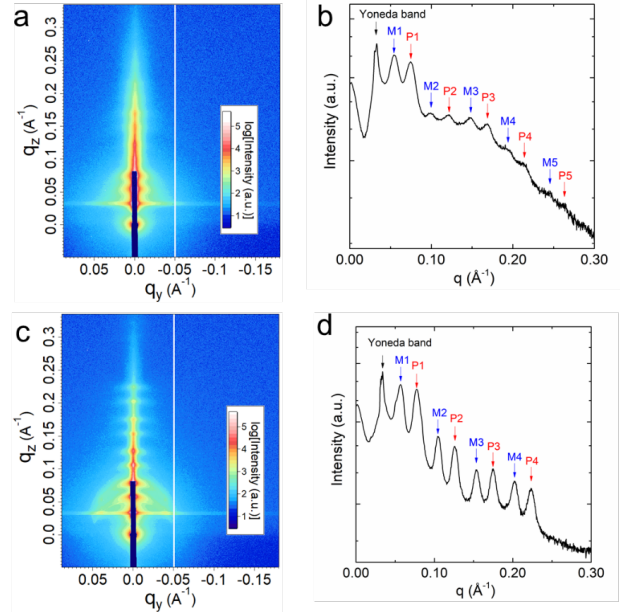
membranes (see details in supporting information). Briefly, a waten-soluble sacrificial laver was first spin coated on UV-ozone treated silicon wafer substrate using an aqueous poly(3,4ethylenedioxythiophene)-poly(styrene sulfonate) (PEDOT PSS) dispersion. A polymer-channel solution containing photoinitiator (diphenyl(2.4.6trimethylbenzoyl)phosphine oxide, TMDPO) and cross-linker (pentaerythritol tetrakis(3mercaptopropionate), tetra-SH) dissolved in THF was then spin coated on top of the PEDOT:PSS olaver. 4 The membrane lavers formed as a result of emperature is process were then crosslinker dounder UV light (365 nm) through thiol-ene click chemistry. Finally, the substrate was immersed into water to dissolve the PEDOT:PSS sacrificial layer and detach the lamellar

membrane, which was later transferred to an aluminum oxide porous substrate to afford the

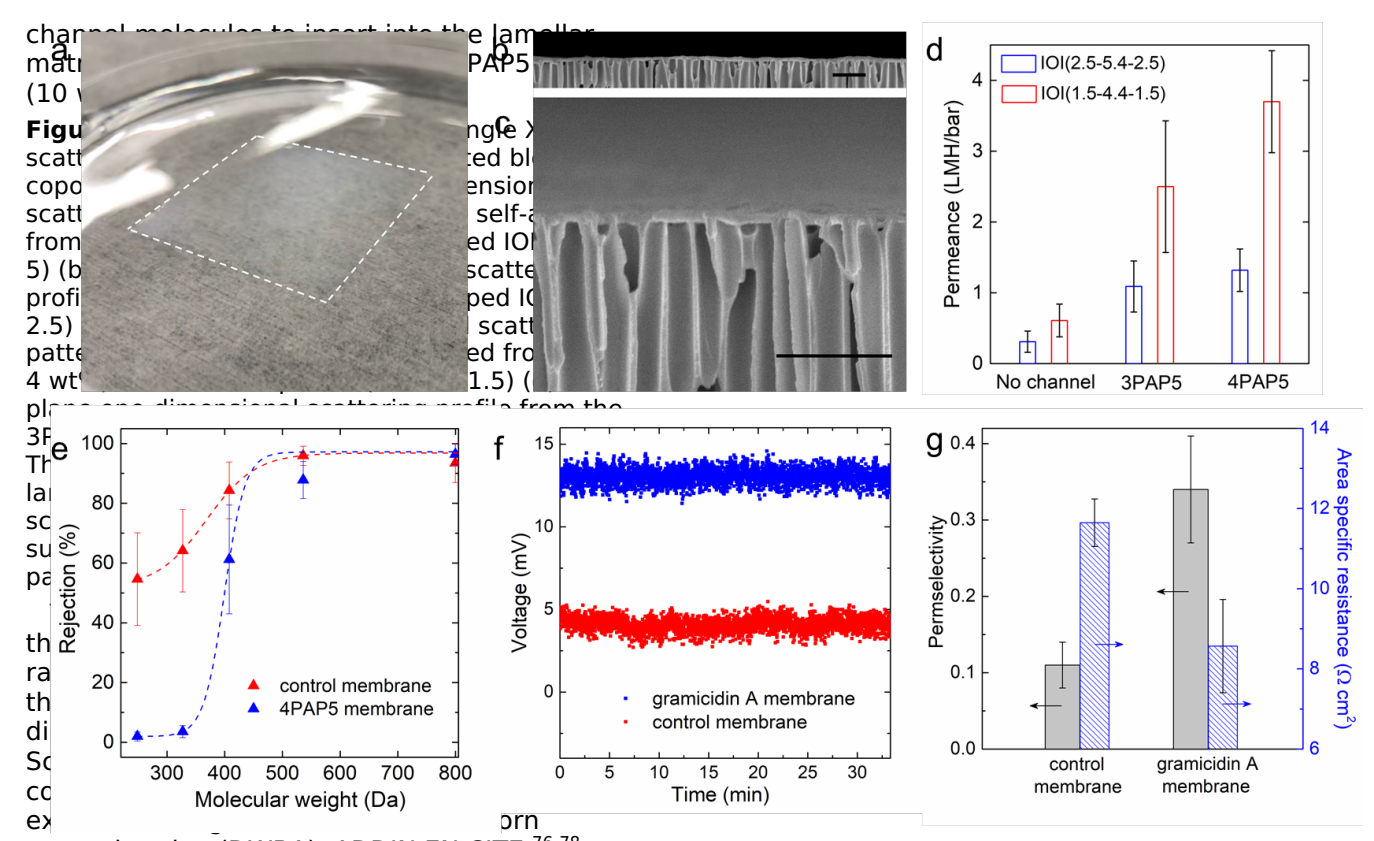
composite membrane.

AFM was used to characterize the surface morphology of the lamellar structures created via spin-coating (Figure 3). Thin film samples from IOI triblock copolymers on silica substrates (before detachment) were used for imaging. Initial results on pure IOI(2.5-5.4-2.5) film showed that. although lamellar structures can be readily created, many micron-scale defects were observed (Figure 3a). As seen from the corresponding height profile (Figure 3d), up to 9 different consecutive height steps parallel to the substrate can be distinguished from the substrate surface to the top of the film. Furthermore, two types of materials exhibiting different adhesion forces with the AFM tip were observed (Figure **\$10**). The polymer coated area exhibited a smaller adhesion force with the tip, while the uncovered area (hard substrate) exhibited a larger force, indicating defects. The formation of these micron-sized defects was attributed to the semi-crystalline nature of PEO where continuous coverage of substrate by polymer self-assembly is interrupted by polymer crystallization. It is known lithium bis(trifluoromethanesulfonyl) imide (LiTFSI) can suppress the crystallization behavior of PEO.⁶⁹ To confirm this known trend⁶⁹ in our system, differential scanning calorimetry (DSC) was used to characterize the thermal behavior of the block copolymer and LiTFSI complex (Figure **3q, 3h**). A distinct endothermic peak was observed around 50°C for the pure polymer during the second heating ramp, which corresponds to the melting peak of PEO crystalline region. The crystallinity of the polymer was calculated to be 37.3% using the heat of

fusion value for an infinite PEO crystal with Equation (S2).⁷⁰ Increasing concentration of salt (



expressed as [Li]:[EO], molar ratio between LiTFSI and EO unit in the polymer) led to decrease in both the crystallinity and melting temperature (T _m) of the polymer (**Figure 3g**). At [Li]:[EO] = 0.1, the crystallization peak was not detectable, indicating that under these conditions a majority of the PEO domains are amorphous (Figure 3h). The LiTFSI ratio, [Li]:[EO] = 0.1, was thus selected to fabricate all the lamellar membranes used in the study. As characterized by AFM, the surface of the lamellar films became flat and free of detectable defects by using LiTFSI doped IOI (Figure 3b, S10). The height profile of the membrane surface showed 3 continuous layers. Compared with 1 D_{lam} (domain spacing values of the lamellar) thick steps observed in the LiTFSI doped IOI film (Figure 3e, S9f, Table S1), pure IOI film exhibits 0.5 D_{lam} thick steps (**Figure 3d**, **S9d**), which is typically formed under kinetic control.⁷¹ Meanwhile, the AFM adhesion force image has shown the surface only consists of one material (Figure 3c). A representative AFM image of a three-layer-step lamellar from IOI(2.5-5.4-2.5) is shown in **Figure 3b** and **3c**. The lamellar structure can also be confirmed with angle-resolved X-ray photoelectron spectroscopy (XPS). At a "surface angle" of 30°, a hydrocarbonrich layer was discovered while at a "bulk angle" of 85°, a sub-layer enriched in C-O was indicated (Figure S11). The results indicate that the obtained lamellar structure is parallel to the substrate surface and the top layer of the lamellae is poly(isoprene), due to its lower surface energy compared to PEO. ADDIN EN.CITE 72-74 Confocal microscopy was also performed on the thin film sample to confirm the ability of



approximation (DWBA). ADDIN EN.CITE $^{76-78}$ Orientation of the lamellae can be determined from the intensity distribution of the DDRs, where strong intensity along the q_z direction indicates lamellae parallel to the substrate. After doping with LiTFSI and adding channel molecules, both IOI(2.5-5.4-2.5) and IOI(1.5-4.4-1.5) films exhibit multiple reflections along q_z , indicating well-ordered lamellar structures parallel to the substrate (**Figure 4a, 4c**). The out-of-plane one-dimensional scattering profile was obtained by averaging scattering intensities from two-dimensional patterns (**Figure 4b, 4d**).

Using DWBA, ADDIN EN.CITE $^{76-78}$ the position of scattering peaks along q_z direction (peaks in out-of-plane scattering profiles) can yield determine D_{lam} with Equation (S3) (see more details in SI). We find domain spacing values for LiTFSI doped IOI(2.5-5.4-2.5) and IOI(1.5-4.4-1.5) of 14.1 nm and 12.5 nm, respectively, which are consistent with height values observed in AFM micrographs (**Table S1**).

Figure 5. Channel-based lamellar membrane structure and performance characterization. (a) The fabricated lamellar membrane can be floated onto water and transferred to other substrates. (b, c) Cross-section scanning electronic microscope (SEM) image of the channel lamellar membrane transferred on to a porous aluminum oxide support. Scale bar: 1 μ m. (d) Water permeance of lamellar composite membrane fabricated with and without artificial channels (15 wt%). (e) Rejection profiles of IOI(1.5-4.4-1.5) lamellar membrane with and without 15 wt% 4PAP5 channels determined by a range of small molecular weight dyes (Table S2). The control membrane was fabricated using the same method and condition as the channel membrane without adding channel molecules. (f) Measured potentials of IOI(1.5-4.4-1.5) lamellar membranes with and without gramicidin A (gA) (15 wt%) upon separating solutions containing high concentration (0.5 M) and low concentration (0.1 M) of NaCl. (g) Permselectivity and area specific resistance of IOI(1.5-4.4-1.5) lamellar membranes with and without 15 wt% gA.

Finally, to characterize the transport properties of channel-based membranes, the cross-linked

lamellar thin film was floated off the silica substrate by dissolving the sacrificial layer in

water and transferring the thin film onto an aluminum oxide support to form a composite membrane. It was found that the membrane fabricated with IO diblock copolymer frequently tore and delaminated on immersion into water (**Figure S15**), while the self-supporting IOI triblock copolymer membrane remained stable (**Figure 5a**).

Scanning electron microscopy (SEM) was used to characterize the morphology of the composite membrane. Polymer films with an average thickness of about 90 nm with no visible defects at the resolution of the SEM were observed on top of the inorganic substrate (Figure 5b, S16). The separation performance of the lamellar membrane was evaluated using water solutions of a range of small molecular weight dye molecules (249 Da - 3000 Da, Table S2) in a dead end stirred cell filtration system with a membrane size of 25 mm in diameter. We first evaluated the performance of the control membrane, which is fabricated using the same method and condition as the channel membrane but without adding channel molecules. It was found the control membrane exhibits a broad pore distribution size with a molecular weight cut off (MWCO, corresponding to MW of model solute rejected at 90% under testing conditions) around 1900 Da (Figure S17), which was attributed to the presence of defects ADDIN EN.CITE 79-80 in the polymer lamellar membrane matrix. To block these defects, a previously proposed sealing strategy was adopted.81-82 The membrane was filtered with 10 ml of sealing solution (0.02 wt% of Irgacure D-2959 and 0.06 wt% of 1,4benzenedithiol in 75% ethanol aqueous solution) at 30 psi prior to exposure to UV at 365 nm for 30 min. After the sealing process, the water permeance of IOI(1.5-4.4-1.5) membrane decreased from 10.2 LMH/bar to 0.61 LMH/bar, suggesting the membrane becomes much tighter. This sealing procedure was also consistent with the significantly increased rejection performance of the control membrane (Figure 5e).

The separation performance of channel inserted lamellar membrane was then investigated. As expected, the water permeance of channel inserted lamellar membranes was significantly higher than control membranes (**Figure 5d**). Noticeably, the channel inserted IOI(2.5-5.4-2.5) membranes have higher permeance than channel inserted IOI(1.5-4.4-1.5) membranes for both 3PAP5 and 4PAP5, which is attributed to a thicker polyisoprene layer (6.1 nm compared to 4.4 nm, **Table S1**). Not only is a thicker poly(isoprene) layer less permeable to water, it also introduces a physical mismatch between the hydrophobic

domain of the membrane and the channels. At 15 wt%. 4PAP5 inserted IOI(1.5-4.4-1.5) lamellar membrane exhibited a high water permeance of 3.7 LMH/bar (~6 fold increase compared to control membrane), which is similar to commercial nanofiltration membrane permeance at the MWCO of these membranes. 9 Rejection tests of the assembled channel-incorporated lamellar membranes show that with 4PAP5 channels added, the membranes became much more permeable to small molecular weight molecules and displayed a sharp transition in molecular exclusion between MWs of 350 Da and 500 Da. By fitting the selectivity data with a sigmoidal function,⁹ the molecular weight cut-off (MWCO) of the membrane was estimated to be \sim 450 Da, which is consistent with previously reported results with both molecular characterization of transport of PAP5 in lipid vesicles and in nanosheet based polymer membranes.9

To show the versatility and broad applicability of the platform, a natural peptide channel gramicidin A (gA) was also utilized as a separation element to fabricate channel-based cation exchange membrane. As crucial components of various electrochemical separation and energy-related technologies.83 ion exchange membranes allow passage of ionic current via selective transport of charged ions of one type while rejecting the other type. It is known that gA channels exhibit high selectivity of monovalent cations over anions. In model lipid membrane, gA conduct K^+ at the order of $\sim 10^7$ ions per second while excluding anions.84 Furthermore, this selectivity is obtained using a mechanism that does not rely on fixed charges such as that exploited in all commercial ion exchange membranes. 83, 85 To synthesize gA channel based lamellar membranes, the same fabrication process for PAP5-based membrane was successfully applied here with gA. Electrotransport measurements were performed on the fabricated membranes. Using a previously described 4-point direct current method, 86-87 the area specific resistance of the membrane inside a 0.5 M NaCl solution was measured. It was found the gA membrane exhibited a resistance value of 8.6 Ω cm² (**Figure 5g**), which is comparable to commercial membranes.88 In comparison, the control membrane exhibited a higher resistance of 11.6 Ω cm², suggesting that gA channels may help facilitate ions to pass through the membrane matrix. Another important performance parameter, apparent permselectivity of the membrane was determined through the measurement of potential gradient across the membrane when separating 0.5 M and 0.1 M NaCl solutions. By adding gA, the membrane potential

increased more than 3 times from 4.0 mV to 13.1 mV (**Figure 5f**). Presumably, gA channels can serve as separation elements that selectively transport cations over anions across the membrane. More systematic study is needed to further understand and optimize gA-based membranes. Although the permselectivity of the current gA membrane at 0.34 (**Figure 5g**) is not as high as commercial membranes (which are around 0.86 to 0.99),⁸⁸ we propose that increasing the concentration of gA as well as sealing small defects within the lamellar layers would allow for a much greater enhancement of permselectivity across these ion exchange membranes.

CONCLUSION

Through the co-assembly of artificial or natural channels with block copolymers, a method for fabricating channel-based membranes utilizing parallel lamellar structures was developed. With a counterintuitive BAB triblock copolymer design and suppression of the crystallinity of the polymer, a mechanically tough and macro-defect free membrane matrix for channel incorporation was successfully developed. By isolating membrane matrix (block copolymer) and separation element (channel molecules), the separation performance of the membrane can be well controlled at the molecular level. Compared with previously reported layer-by-layer method based on 2D crystals,9 the method described here is much easier, more scalable and doesn't require elongated preparation time. More importantly, we have shown this developed platform can be implemented with different channels (artificial and natural), to target membranes with different functionalities and mechanisms (size exclusion and ion exchange). This platform is beneficial for developing membranes with highly specialized functions enabled by biological and artificial channels, thereby enabling applications ranging from desalination, energy harvesting from salinity gradients, and sensors to bioelectronic devices.

EXPERIMENTAL METHODS

Materials

Monomers for polymerization (MilliporeSigma Corporate, MO) were purified with n-butyllithium (MilliporeSigma Corporate, MO). Organic solvents were used directly from a solvent drying system (JC Meyer Solvent Systems). The polymerization of monomer isoprene was initiated using secbutyllithium (MilliporeSigma Corporate, MO). Potassium naphthalenide solutions used for poly(ethylene oxide) polymerization were prepared 24 h before the initiation of the polymerization. Other commercially available chemicals were used as received. Nuclear magnetic resonance (NMR) experiments were performed on an Avance

AV3HD 500 NMR spectrometer (Bruker) at room temperature. All the obtained spectra were calibrated according to the residual solvent peak. Mass spectroscopy (MS) was performed on a Bruker ultrafleXtreme MALDI-TOF. The size-exclusion chromatography (SEC) experiments were performed on an EcoSEC HLC-8320GPC (Tosoh Bioscience) equipped with a DAWN multi-angle light scattering (MALS) detector (Wyatt Technology).

Membrane fabrication

A typical membrane fabrication method was as follows: clean silicon wafers (Process Specialties Inc., CA) were thoroughly washed with acetone, THF and ethanol in turn followed by air blown to dry. The wafers were then treated with UV-ozone (UVO-Cleaner®, Jelight Company Inc., CA) to obtain a hydrophilic surface, followed by spin coating (4000 rpm/min) of a water-soluble sacrificial layer using poly(3,4ethylenedioxythiophene)-poly(styrene sulfonate) (PEDOT:PSS) solution (Clevios™ P, Heraeus, Germany) on to the substrate. A polymer-channel THF solution with the following content was then prepared: 20 mg/ml of IOI(2.5-5.4-2.5) or IOI(1.5-4.4-1.5) with LiTFSI ([Li]:[EO]=0.1) and desired amount of channel molecules: 0.4 mg/ml of photoinitiator (diphenyl(2,4,6-trimethylbenzoyl) phosphine oxide, TMDPO) and 1.6 mg/ml

of cross-linker (pentaerythritol tetrakis(3-mercaptopropionate), tetra-SH). The solution was filtered through a 0.22 µm filter and spin coated (1000 rpm/min) on top of the PEDOT:PSS layer. The membrane layers formed as a result of this process were then crosslinked under UV light (365 nm) for 45 min through thiol-ene click chemistry. Finally, the substrate was soaked in water to dissolve the PEDOT:PSS sacrificial layer and detach the lamellar membrane, which was later transferred to an aluminum oxide porous substrate (Whatman®, MilliporeSigma Corporate, MO) to afford the composite membrane.

Characterization

Atomic force microscopy (AFM). AFM measurements were performed on a Dimension Icon (Bruker) AFM microscope using PeakForce Tapping mode. A triangular shaped ScanAsyst-Air tip with a tip radius of 2-12 nm was used in this study. The laser alignment was performed by tuning the sum value to a maximum. During the measurement, the peak force setpoint was set to 500.0 pN. To collect a typical image, the scan was performed at a scan rate of 0.977 Hz and 512 lines per sample. Lamellar thin film samples on silicon substrates were used for AFM characterization. The accuracy of the image was confirmed by checking the trace and retrace peak force curve and comparing the AFM data from trace and retrace channels. Retrace images are used in the paper.

X-ray photoelectron spectroscopy (XPS). XPS experiments were performed using a Physical Electronics VersaProbe II instrument equipped with a monochromatic Al $k\alpha$ x-ray source ($h\nu$ = 1486.7 eV) and a concentric hemispherical analyzer. Charge neutralization was performed using both low energy electrons (<5 eV) and argon ions. The binding energy axis was calibrated using sputter cleaned Cu (Cu $2p_{3/2}$ = 932.62 eV, Cu $3p_{3/2} = 75.1$ eV) and Au foils (Au 4f $_{7/2}$ = 83.96 eV). Peaks were charge referenced to CHx band in the carbon 1s spectra at 284.8 eV. Measurements were made at takeoff angles of 30° and 85° with respect to the sample surface plane. This resulted in a typical sampling depth of 2-4 nm and 4-7 nm (95% of the signal originated from this depth or shallower), respectively. Quantification was done using instrumental relative sensitivity factors (RSFs) that account for the x-ray cross section and inelastic mean free path of the electrons.

Grazing-incidence small angle X-ray scattering (GISAXS). The structure, orientation and domain spacing of polymer thin films were characterized by GISAXS at beamline 7.3.3 of the Advanced Light Source at Lawrence Berkeley National Laboratory.⁸⁹ To perform GISAXS measurements, thin films spun-cast from premixed polymer

solutions without photoinitiator and cross-linker on UV-Ozone treated silica substrates were used. Data was collected using a 2M Pilatus detector with a sample to detector distance of 3 meters. The incident X-ray has an energy of 10 keV ($\lambda=1.24$ Å). At this energy, the critical angle of the film (α CP) and the substrate (α CSi) was 0.125° and 0.18°, respectively. An incident angle of 0.175° was used to sample the bulk film. The out-of-plane scattering profile was obtained using Igor Nika package⁹⁰ by by averaging the scattering intensity with a q window of 0.00595 Å-1< $q_{x,y}$ < 0.01445 Å-1.

Scanning electron microscope (SEM). A FEI Nova NanoSEM 630 FESEM scanning electron microscope (SEM) was used to characterize the composite membrane. The membranes were dried, sputtered with 8 nm iridium (Leica EM ACE600, Germany) and then characterized on SEM at 5 keV. The support membrane is Whatman® Anodisc inorganic filter membrane with a diameter of 25 mm and pore size of 0.2 μm

ACKNOWLEDGEMENT

This work was primarily funded by National Science Foundation (NSF) grant CBET-1262 1552571 and US Army CERL W9132T-16-2-12640004-P00003. This work was also supported using start-up funds from the Penn State University to RIH. The GISAXS characterization used resources of the Advanced Light Source, which is a DOE Office of Science User Facility under contract no. DE-AC02-05CH11231. The authors acknowledge Eric Schaible for the help with GISAXS measurement. AFM, SEM and XPS measurements were taken at the Materials Characterization Lab (MCL) in the Materials Research Institute (MRI) at Penn State University. We thank Tim Tighe for the help with AFM and Jeff Shallenberger for the XPS measurement and analysis.

ASSOCIATED CONTENT

Synthesis and characterization of the channels and polymers, preparation of vesicles, details of stopped -flow, FCS, DSC, XPS, Confocal microscopy, lamellar spacing calculations, and membrane performance characterizations are included in the supplemental information. This material is available free of charge *via* the Internet at http://pubs.acs.org.

AUTHOR INFORMATION

Corresponding Author

*E-mail: manish.kumar@psu.edu. E-mail: rjh64@psu.edu.

REFERENCE

ADDIN EN.REFLIST (1) Robeson, L. M., The

Upper Bound Revisited. J. Membr. Sci. 2008, 320, 390-

400.

- (2) Mehta, A.; Zydney, A. L., Permeability and Selectivity Analysis for Ultrafiltration Membranes. *J. Membr. Sci.* **2005**, *249*, 245-249.
- (3) Werber, J. R.; Osuji, C. O.; Elimelech, M., Materials for Next-Generation Desalination and Water Purification Membranes. *Nat. Rev. Mater.* **2016**, *1*, 16018.
- (4) Park, H. B.; Kamcev, J.; Robeson, L. M.; Elimelech, M.; Freeman, B. D., Maximizing the Right Stuff: The Trade -Off Between MembraneOpermeability and Selectivity. *Science* **2017**, *356*, eaab0530.
- (5) Shen, Y.-x.; Saboe, P. O.; Sines, I. T.; Erbakan, M.; Kumar, M., Biomimetic Membranes: A Review. *J. Membr* . *Sci.* **2014**, *454*, 359-381.
- (6) Agre, P., Aquaporin Water Channels (Nobel lecture). *Angew. Chem., Int. Ed.* **2004,** 43, 4278-4290.

- (7) de Groot, B. L.; Grubmüller, H., Water Permeation Across Biological Membranes: Mechanism and Dynamics of Aquaporin-1 and GlpF. *Science* **2001,** *294*, 2353-2357.
- (8) Hille, B., *Ion Channels of Excitable Membranes*. Sinauer Sunderland, MA: 2001; Vol. 507.
- (9) Shen, Y.-x.; Song, W. C.; Barden, D. R.; Ren, T.; Lang, C.; Feroz, H.; Henderson, C. B.; Saboe, P. O.; Tsai, D.; Yan, H., Achieving High Permeability and Enhanced Selectivity for Angstrom-Scale Separations Using Artificial Water Channel Membranes. *Nat. Commun.* **2018**, *9*:2294.
- (10) Clarke, J.; Wu, H.-C.; Jayasinghe, L.; Patel, A.; Reid, S.; Bayley, H., Continuous Base Identification for Single-Molecule Nanopore DNA Sequencing. *Nat. Nanotechnol.* **2009,** *4*, 265-270.
- (11) Burns, J. R.; Al-Juffali, N.; Janes, S. M.; Howorka, S., Membrane-Spanning DNA Nanopores with Cytotoxic Effect. *Angew. Chem., Int. Ed.* **2014,** *53*, 12466-12470. (12) Boersma, A. J.; Brain, K. L.; Bayley, H., Real-Time Stochastic Detection of Multiple Neurotransmitters wth a Protein Nanopore. *ACS Nano* **2012,** *6*, 5304-5308. (13) Misra, N.; Martinez, J. A.; Huang, S.-C. J.; Wang, Y.; Stroeve, P.; Grigoropoulos, C. P.; Noy, A., Bioelectronic Silicon Nanowire Devices Using Functional Membrane Proteins. *Proc. Natl. Acad. Sci. U. S. A.* **2009,** *106*,
- (14) Guan, X.; Gu, L. Q.; Cheley, S.; Braha, O.; Bayley, H., Stochastic Sensing of TNT with a Genetically Engineered Pore. *ChemBioChem* 2005, 6, 1875-1881.
 (15) Carter, J.-M.; Hussain, S., Robust Long-Read Native DNA Sequencing Using the ONT CsgG Nanopore System. *Wellcome Open Res.* 2017, 2:23.

13780-13784.

- (16) Fane, A. G.; Wang, R.; Hu, M. X., Synthetic Membranes for Water Purification: Status and Future. *Angew. Chem., Int. Ed.* **2015,** *54*, 3368-3386. (17) Kumar, M.; Habel, J. E.; Shen, Y.-x.; Meier, W. P.; Walz, T., High-Density Reconstitution of Functional Water Channels into Vesicular and Planar Block Copolymer Membranes. *J. Am. Chem. Soc.* **2012,** *134*, 18631-18637.
- (18) Palivan, C. G.; Goers, R.; Najer, A.; Zhang, X.; Car, A.; Meier, W., Bioinspired Polymer Vesicles and Membranes for Biological and Medical Applications.

- Chem. Soc. Rev. 2016, 45, 377-411.
- (19) Matile, S.; Jentzsch, A. V.; Montenegro, J.; Fin, A., Recent Synthetic Transport Systems. *Chem. Soc. Rev.* **2011**, *40*, 2453-2474.
- (20) Barboiu, M., Artificial Water Channels. *Angew. Chem., Int. Ed.* **2012,** *51*, 11674-11676.
- (21) Hu, X.-B.; Chen, Z.; Tang, G.; Hou, J.-L.; Li, Z.-T., Single-Molecular Artificial Transmembrane Water Channels. *J. Am. Chem. Soc.* **2012**, *134*, 8384-8387.
- (22) Zhou, X.; Liu, G.; Yamato, K.; Shen, Y.; Cheng, R.; Wei, X.; Bai, W.; Gao, Y.; Li, H.; Liu, Y.; Liu, F.;
- Czajkowsky, D. M.; Wang, J.; Dabney, M. J.; Cai, Z.; Hu, J.; Bright, F. V.; He, L.; Zeng, X. C.; Shao, Z.; Gong, B.,
- Self-Assembling Subnanometer Pores with Unusual Mass-Transport Properties. *Nat. Commun.* **2012**, *3:949*.
- (23) Lang, C.; Deng, X.; Yang, F.; Yang, B.; Wang, W.; Qi
- , S.; Zhang, X.; Zhang, C.; Dong, Z.; Liu, J., Highly Selective Artificial Potassium Ion Channels Constructed
- from Pore-Containing Helical Oligomers. *Angew. Chem.* **2017**, *129*, 12842-12845.
- (24) Fyles, T. M., Synthetic Ion Channels in Bilayer Membranes. *Chem. Soc. Rev.* **2007,** *36*, 335-347.
- (25) Kawano, R.; Horike, N.; Hijikata, Y.; Kondo, M.; Carné-Sánchez, A.; Larpent, P.; Ikemura, S.; Osaki, T.; Kamiya, K.; Kitagawa, S., Metal-Organic Cuboctahedra for Synthetic Ion Channels with Multiple Conductance

States. Chem 2017, 2, 393-403.

- (26) Langecker, M.; Arnaut, V.; Martin, T. G.; List, J.; Renner, S.; Mayer, M.; Dietz, H.; Simmel, F. C., Synthetic Lipid Membrane Channels Formed by Designed DNA Nanostructures. *Science* **2012**, *338*, 932 -936.
- (27) Howorka, S., Building Membrane Nanopores. *Nat. Nanotechnol.* **2017**, *12*, 619-630.
- (28) Tunuguntla, R. H.; Henley, R. Y.; Yao, Y.-C.; Pham, T. A.; Wanunu, M.; Noy, A., Enhanced Water Permeability and Tunable Ion Selectivity in Subnanometer Carbon Nanotube Porins. *Science* **2017**, *357*, 792-796.
- (29) Hou, X.; Guo, W.; Jiang, L., Biomimetic Smart Nanopores and Nanochannels. *Chem. Soc. Rev.* **2011,** *40*, 2385-2401.
- (30) Si, W.; Xin, P.; Li, Z.-T.; Hou, J.-L., Tubular Unimolecular Transmembrane Channels: Construction

- Strategy and Transport Activities. *Acc. Chem. Res.* **2015**, *48*, 1612-1619.
- (31) Matile, S.; Fyles, T., Transport Across Membranes. *Acc. Chem. Res.* **2013**, *46*, 2741-2742.
- (32) Lang, C.; Li, W.; Dong, Z.; Zhang, X.; Yang, F.; Yang, B.; Deng, X.; Zhang, C.; Xu, J.; Liu, J., Biomimetic Transmembrane Channels with High Stability and Transporting Efficiency from Helically Folded Macromolecules. *Angew. Chem., Int. Ed.* **2016,** *55*, 9723-9727.
- (33) Rilfors, L.; Lindblom, G.; Wieslander, Å.; Christiansson, A., Lipid Bilayer Stability in Biological Membranes. In *Membrane Fluidity*; Kates, M., Ed.; Springer: Boston, 1984; pp 205-245.
- (34) Kumar, M.; Grzelakowski, M.; Zilles, J.; Clark, M.; Meier, W., Highly Permeable Polymeric Membranes Based on the Incorporation of The Functional Water Channel Protein Aquaporin Z. *Proc. Natl. Acad. Sci. U. S. A.* **2007**, *104*, 20719-20724.
- (35) Duong, P. H.; Chung, T.-S.; Jeyaseelan, K.; Armugam, A.; Chen, Z.; Yang, J.; Hong, M., Planar Biomimetic Aquaporin-Incorporated

- Triblock Copolymer Membranes on Porous Alumina Supports for Nanofiltration. *J. Membr. Sci.* **2012,** *409,* 34-43.
- (36) Wang, H.; Chung, T. S.; Tong, Y. W.; Jeyaseelan, K.; Armugam, A.; Chen, Z.; Hong, M.; Meier, W., Highly Permeable and Selective Pore-spanning Biomimetic Membrane Embedded with Aquaporin Z. *Small* **2012**, *8*, 1185-1190.
- (37) Klara, S. S.; Saboe, P. O.; Sines, I. T.; Babaei, M.; Chiu, P.-L.; DeZorzi, R.; Dayal, K.; Walz, T.; Kumar, M.; Mauter, M. S., Magnetically Directed Two-Dimensional Crystallization of OmpF Membrane Proteins in Block Copolymers. *J. Am. Chem. Soc.* **2015**, *138*, 28-31.
- (38) Discher, B. M.; Won, Y.-Y.; Ege, D. S.; Lee, J. C.; Bates, F. S.; Discher, D. E.; Hammer, D. A., Polymersomes: Tough Vesicles Made From Diblock Copolymers. *Science* **1999**, *284*, 1143-1146.
- (39) Discher, D. E.; Eisenberg, A., Polymer Vesicles. *Science* **2002**, *297*, 967-973.
- (40) Meier, W.; Nardin, C.; Winterhalter, M., Reconstitution of Channel Proteins in Polymerized ABA Triblock Copolymer Membranes. *Angew. Chem., Int. Ed.* **2000,** *39*, 4599-4602.
- (41) Shen, Y.-x.; Si, W.; Erbakan, M.; Decker, K.; De Zorzi, R.; Saboe, P. O.; Kang, Y. J.; Majd, S.; Butler, P. J.; Walz, T., Highly Permeable Artificial Water Channels that Can Self-assemble into Two-Dimensional Arrays. *Proc. Natl. Acad. Sci. U. S. A.* 2015, 112, 9810-9815.
 (42) Mai, Y.; Eisenberg, A., Self-Assembly of Block Copolymers. *Chem. Soc. Rev.* 2012, 41, 5969-5985.
 (43) Bates, F. S.; Fredrickson, G., Block Copolymers-DesignerSsoft Materials. *Phys. Today* 2000, 52, 32-38.
 (44) Albert, J. N.; Epps III, T. H., Self-Assembly of Block Copolymer Thin Films. *Mater. Today* 2010, 13, 24-33.
 (45) Epps III, T. H.; O'Reilly, R. K., Block Copolymers: Controlling Nanostructure to Generate Functional Materials-Synthesis, Characterization, and Engineering. *Chem. Sci.* 2016, 7, 1674-1689.
- (46) Feng, X.; Tousley, M. E.; Cowan, M. G.; Wiesenauer, B. R.; Nejati, S.; Choo, Y.; Noble, R. D.; Elimelech, M.; Gin, D. L.; Osuji, C. O., Scalable Fabrication of Polymer Membranes with Vertically Aligned 1 nm Pores by Magnetic Field Directed Self-Assembly. *ACS Nano* **2014**, *8*, 11977-11986.

- (47) Feng, X.; Nejati, S.; Cowan, M. G.; Tousley, M. E.; Wiesenauer, B. R.; Noble, R. D.; Elimelech, M.; Gin, D. L.; Osuji, C. O., Thin Polymer Films with Continuous Vertically Aligned 1 nm Pores Fabricated by Soft Confinement. *ACS Nano* **2015**, *10*, 150-158.

 (48) Feng, X.; Kawabata, K.; Kaufman, G.; Elimelech, M.; Osuji, C. O., Highly Selective Vertically Aligned Nanopores in Sustainably Derived Polymer Membranes by Molecular Templating. *ACS Nano* **2017**, *11*, 3911-3921.
- (49) Nunes, S. P., Block Copolymer Membranes for Aqueous Solution Applications. *Macromolecules* **2016**, *49*, 2905-2916.
- (50) Hu, H.; Gopinadhan, M.; Osuji, C. O., Directed Self-Assembly of Block Copolymers: a Tutorial Review of Strategies for Enabling Nanotechnology with soft matter. *Soft matter* **2014**, *10*, 3867-3889.
- (51) Jackson, E. A.; Hillmyer, M. A., Nanoporous Membranes Derived From Block Copolymers: From Drug Delivery To Water Filtration. *ACS Nano* **2010**, *4*, 3548-3553.
- (52) Peinemann, K.-V.; Abetz, V.; Simon, P. F., Asymmetric Superstructure Formed in a Block Copolymer *via* Phase separation. *Nat. Mater.* **2007,** *6*, 992.
- (53) Abetz, V., Isoporous Block Copolymer Membranes. *Macromol. Rapid Commun.* **2015**, *36*, 10-22.
- (54) Phillip, W. A.; Dorin, R. M.; Werner, J. r.; Hoek, E. M.; Wiesner, U.; Elimelech, M., Tuning Structure and Properties of Graded Triblock Terpolymer-Based Mesoporous and Hybrid Films. *Nano Lett.* **2011,** *11*, 2892-2900.
- (55) Pitet, L. M.; Amendt, M. A.; Hillmyer, M. A., Nanoporous Linear Polyethylene From a Block Polymer Precursor. *J. Am. Chem. Soc.* **2010**, *132*, 8230-8231. (56) Seo, M.; Hillmyer, M. A., Reticulated Nanoporous Polymers by Controlled Polymerization-induced Microphase Separation. *Science* **2012**, *336*, 1422-1425. (57) Song, L.; Feng, D.; Fredin, N. J.; Yager, K. G.; Jones, R. L.; Wu, Q.; Zhao, D.; Vogt, B. D., Challenges in Fabrication of Mesoporous Carbon Films with Ordered Cylindrical Pores *via* Phenolic Oligomer Self-assembly with Triblock Copolymers. *ACS Nano* **2009**, *4*, 189-198.

- (58) Labiano, A.; Dai, M.; Young, W.-S.; Stein, G. E.; Cavicchi, K. A.; Epps III, T. H.; Vogt, B. D., Impact of Homopolymer Pore Expander on the Morphology of Mesoporous Carbon Films Using Organic-Organic Self-Assembly. *J. Phys. Chem. C* **2012**, *116*, 6038-6046. (59) Yu, H.; Qiu, X.; Moreno, N.; Ma, Z.; Calo, V. M.; Nunes, S. P.; Peinemann, K. V., Self-Assembled Asymmetric Block Copolymer Membranes: Bridging the Gap From Ultra-To Nanofiltration. *Angew. Chem., Int. Ed*. **2015**, *54*, 13937-13941.
- (60) Yu, H.; Qiu, X.; Nunes, S. P.; Peinemann, K. V., Self-Assembled Isoporous Block Copolymer Membranes with Tuned Pore Sizes. *Angew. Chem., Int. Ed.* **2014,** *53*, 10072-10076.
- (61) Zhang, Y.; Mulvenna, R. A.; Qu, S.; Boudouris, B. W.; Phillip, W. A., Block Polymer Membranes
 Functionalized with Nanoconfined Polyelectrolyte
 Brushes Achieve Sub-Nanometer Selectivity. *ACS Macro Lett.* **2017**, *6*, 726-732.
- (62) Chen, Q. P.; Barreda, L.; Oquendo, L. E.; Hillmyer, M. A.; Lodge, T. P.; Siepmann, J. I., Computational Design of High-χ Block

- Oligomers for Accessing 1 nm Domains. *ACS Nano* **2018**, *12*, 4351-4361.
- (63) Song, W.; Lang, C.; Shen, Y.-x.; Kumar, M., Design Considerations for Artificial Water Channel-Based Membranes. *Annu. Rev. Mater. Res.* **2018**, *48*, 57-82. (64) Song, W.; Shen, Y.-x.; Lang, C.; Saha, P.; Zenyuk, I. V.; Hickey, R. J.; Kumar, M., Unique Selectivity Trends of Highly Permeable PAP [5] Water Channel Membranes. *Faraday Discuss.* **2018**, *209*, 193-204.

(65) Xu, T.; Zhao, N.; Ren, F.; Hourani, R.; Lee, M. T.;

Shu, J. Y.; Mao, S.; Helms, B. A., Subnanometer Porous

- Thin Films by the Co-Assembly of Nanotube Subunits and Block Copolymers. *ACS Nano* **2011**, *5*, 1376-1384. (66) Lang, C.; Shen, Y.-x.; LaNasa, J. A.; Ye, D.; Song, W.; Zimudzi, T. J.; Hickner, M. A.; Gomez, E. D.; Gomez, E. W.; Kumar, M., Creating Cross-Linked Lamellar Block Copolymer Supporting Layers for Biomimetic Membranes. *Faraday Discuss.* **2018**, *209*, 179-191. (67) Lee, J. C. M.; Bermudez, H.; Discher, B. M.; Sheehan, M. A.; Won, Y. Y.; Bates, F. S.; Discher, D. E., Preparation, Stability, and *In Vitro* Performance of Vesicles Made with Diblock Copolymers. *Biotechnol.*
- (68) Latimer, P.; Pyle, B., Light Scattering at Various Angles: Theoretical Predictions of the Effects of Particle Volume Changes. *Biophys. J.* **1972,** *12*, 764-773.

Bioeng. 2001, 73, 135-145.

- (69) Benrabah, D.; Baril, D.; Sanchez, J.-Y.; Armand, M.; Gard, G. G., Comparative Electrochemical Study of New Poly (oxyethylene)-Li Salt Complexes. *J. Chem. Soc., Faraday Trans.* **1993,** *89*, 355-359.
- (70) Qiu, Z.; Ikehara, T.; Nishi, T., Miscibility and Crystallization in Crystalline/Crystalline Blends of Poly (Butylene Succinate)/Poly (Ethylene Oxide). *Polymer* **2003**, *44*, 2799-2806.
- (71) Maher, M. J.; Self, J. L.; Stasiak, P.; Blachut, G.; Ellison, C. J.; Matsen, M. W.; Bates, C. M.; Willson, C. G., Structure, Stability, and Reorganization of $0.5 L_0$ Topography in Block Copolymer Thin Films. *ACS Nano* **2016**, *10*, 10152-10160.
- (72) Lee, L. H., Adhesion of High Polymers. II. Wettability of Elastomers. *J. Polym. Sci., Part A-2: Polym. Sci.* **1967,** *5*, 1103-1118.
- (73) Van Oss, C.; Chaudhury, M.; Good, R. J., Monopolar Surfaces. *Adv. Colloid Interface Sci.* **1987**, *28*, 35-64.

- (74) Anastasiadis, S.; Russell, T.; Satija, S.; Majkrzak, C., Neutron Reflectivity Studies of the Surface-Induced Ordering of Diblock Copolymer Films. *Phys. Rev. Lett.* **1989**, *62*, 1852.
- (75) Busch, P.; Posselt, D.; Smilgies, D.-M.; Rauscher, M.; Papadakis, C. M., Inner Structure of Thin Films of Lamellar Poly (Styrene-b-Butadiene) Diblock Copolymers as Revealed by Grazing-Incidence Small-Angle Scattering. *Macromolecules* **2007**, *40*, 630-640. (76) Busch, P.; Rauscher, M.; Smilgies, D.-M.; Posselt, D.; Papadakis, C. M., Grazing-Incidence Small-Angle X-Ray Scattering From Thin Polymer Films with Lamellar Structures-the Scattering Cross Section in the Distorted -Wave Born Approximation. *J. Appl. Crystallogr.* **2006**, *39*, 433-442.
- (77) Zhang, J.; Posselt, D.; Smilgies, D.-M.; Perlich, J.; Kyriakos, K.; Jaksch, S.; Papadakis, C. M., Lamellar Diblock Copolymer Thin Films During Solvent Vapor Annealing Studied by GISAXS: Different Behavior of Parallel and Perpendicular Lamellae. *Macromolecules* **2014**, *47*, 5711-5718.
- (78) Busch, P.; Rauscher, M.; Moulin, J.-F.; Mueller-Buschbaum, P., Debye-Scherrer Rings from Block Copolymer Films with Powder-Like Order. *J. Appl. Crystallogr.* **2011**, *44*, 370-379.
- (79) O'Hern, S. C.; Stewart, C. A.; Boutilier, M. S.; Idrobo, J.-C.; Bhaviripudi, S.; Das, S. K.; Kong, J.; Laoui, T.; Atieh, M.; Karnik, R., Selective Molecular Transport Through Intrinsic Defects in a Single Layer of CVD Graphene. *ACS Nano* **2012**, *6*, 10130-10138.
- (80) Boutilier, M. S.; Sun, C.; O'Hern, S. C.; Au, H.; Hadjiconstantinou, N. G.; Karnik, R., Implications of Permeation Through Intrinsic Defects in Graphene on the Design of Defect-Tolerant Membranes for Gas Separation. *ACS Nano* **2014**, *8*, 841-849.
- (81) O'Hern, S. C.; Jang, D.; Bose, S.; Idrobo, J.-C.; Song, Y.; Laoui, T.; Kong, J.; Karnik, R., Nanofiltration Across Defect-Sealed Nanoporous Monolayer Graphene. *Nano Lett.* **2015**, *15*, 3254-3260.
- (82) Wang, L.; Boutilier, M. S.; Kidambi, P. R.; Jang, D.; Hadjiconstantinou, N. G.; Karnik, R., Fundamental Transport Mechanisms, Fabrication and Potential Applications of Nanoporous Atomically Thin Membranes . *Nat. Nanotechnol.* **2017**, *12*, 509.

- (83) Xu, T., Ion Exchange Membranes: State of Their Development and Perspective. *J. Membr. Sci.* **2005**, *263*, 1-29.
- (84) Hladky, S.; Haydon, D., Ion Transfer Across Lipid Membranes in the Presence of Gramicidin A: I. Studies of the Unit Conductance Channel. *BBA-Biomembranes* **1972**, *274*, 294-312.
- (85) He, G.; Li, Z.; Zhao, J.; Wang, S.; Wu, H.; Guiver, M. D.; Jiang, Z., Nanostructured Ion-Exchange Membranes for Fuel Cells: Recent Advances and Perspectives. *Adv. Mater.* **2015**, *27*, 5280-5295.
- (86) Geise, G. M.; Hickner, M. A.; Logan, B. E., Ionic Resistance and Permselectivity Tradeoffs in Anion Exchange Membrane. *ACS Appl. Mater. Interfaces* **2013**, *5*, 10294-10301.
- (87) Capparelli, C.; Fernandez Pulido, C. R.; Wiencek, R. A.; Hickner, M. A., Resistance and Permselectivity of 3D Printed Micropatterned Anion Exchange Membranes. *ACS Appl. Mater. Interfaces* **2018**, *10.1021/acsami. 8b04177*.

(88) Długołęcki, P.; Nymeijer, K.; Metz, S.; Wessling, M., Current Status of Ion Exchange Membranes for Power Generation from Salinity Gradients. *J. Membr. Sci.* **2008**, *319*, 214-222.

(89) Hexemer, A.; Bras, W.; Glossinger, J.; Schaible, E.; Gann, E.; Kirian, R.; MacDowell, A.; Church, M.; Rude, B.; Padmore, H. In A SAXS/WAXS/GISAXS Beamline with Multilayer Monochromator. *J. Phys. Conf. Ser.* **2010**, 247, 012007.

(90) Ilavsky, J., Nika: Software for Two-Dimensional Data Reduction . *J. Appl. Crystallogr.* **2012**, 45, 324-328.

Table of Contents

